Mass of genes rather than master genes underlie the genomic architecture of amphibian speciation

Christophe Dufresnes[a,b,1], Alan Brelsford[c], Daniel L. Jeffries[d], Glib Mazepa[d,e], Tomasz Suchan[f], Daniele Canestrelli[g], Alfredo Nicieza[h,i], Luca Fumagalli[j,k], Sylvain Dubey[d], Iñigo Martínez-Solano[l], Spartak N. Litvinchuk[m,n], Miguel Vences[o], Nicolas Perrin[d], and Pierre-André Crochet[p]

[a]LASER, College of Biology and Environment, Nanjing Forestry University, Nanjing 210037, China; [b]Department of Animal and Plant Sciences, University of Sheffield, Sheffield S10 2TN, United Kingdom; [c]Department of Evolution, Ecology, and Organismal Biology, University of California, Riverside, CA 92521; [d]Department of Ecology and Evolution, University of Lausanne, 1015 Lausanne, Switzerland; [e]Department of Ecology and Genetics, Evolutionary Biology Center, Uppsala University, 752 36 Uppsala, Sweden; [f]W. Szafer Institute of Botany, Polish Academy of Sciences, 31-512 Kraków, Poland; [g]Department of Ecological and Biological Sciences, Tuscia University, 01100 Viterbo, Italy; [h]Biodiversity Research Institute, University of Oviedo–Principality of Asturias–CSIC, 33600 Mieres, Spain; [i]Department of Organisms and Systems Biology, University of Oviedo, 33003 Oviedo, Spain; [j]Laboratory for Conservation Biology, Department of Ecology and Evolution, University of Lausanne, 1015 Lausanne, Switzerland; [k]University Centre of Legal Medicine Lausanne–Geneva, Lausanne University Hospital and University of Lausanne, 1000 Lausanne 25, Switzerland; [l]Departamento de Biodiversidad y Biología Evolutiva, Museo Nacional de Ciencias Naturales, 28006 Madrid, Spain; [m]Institute of Cytology, Russian Academy of Sciences, 119991 St. Petersburg, Russia; [n]Department of Biology, Dagestan State University, 367008 Makhachkala, Russia; [o]Zoological Institute, Technische Universität Braunschweig, 38106 Braunschweig, Germany; and [p]CEFE, CNRS, Univ. Montpellier, EPHE, IRD, 34090 Montpellier, France

Edited by David B. Wake, University of California, Berkeley, CA, and approved July 6, 2021 (received for review February 27, 2021)

The genetic architecture of speciation, i.e., how intrinsic genomic incompatibilities promote reproductive isolation (RI) between diverging lineages, is one of the best-kept secrets of evolution. To directly assess whether incompatibilities arise in a limited set of large-effect speciation genes, or in a multitude of loci, we examined the geographic and genomic landscapes of introgression across the hybrid zones of 41 pairs of frog and toad lineages in the Western Palearctic region. As the divergence between lineages increases, phylogeographic transitions progressively become narrower, and larger parts of the genome resist introgression. This suggests that anuran speciation proceeds through a gradual accumulation of multiple barrier loci scattered across the genome, which ultimately deplete hybrid fitness by intrinsic postzygotic isolation, with behavioral isolation being achieved only at later stages. Moreover, these loci were disproportionately sex linked in one group (*Hyla*) but not in others (*Rana* and *Bufotes*), implying that large X-effects are not necessarily a rule of speciation with undifferentiated sex chromosomes. The highly polygenic nature of RI and the lack of hemizygous X/Z chromosomes could explain why the speciation clock ticks slower in amphibians compared to other vertebrates. The clock-like dynamics of speciation combined with the analytical focus on hybrid zones offer perspectives for more standardized practices of species delimitation.

cryptic species | Haldane's rule | phylogeography | sex chromosomes | species delimitation

Reproductive isolation (RI) is the cornerstone of speciation—the evolution of diverging populations into separate species. RI is a multidimensional process, influenced by a complex combination of genetic, behavioral, and ecological factors (1), in which postzygotic barriers—the reduction of hybrid fitness by lower fertility or survival—play a decisive part (2, 3). Understanding how and when these barriers prevent hybridization, lineage merging, and ultimately determine speciation versus despeciation is a fundamental topic in evolutionary biology, with important consequences for the cataloging of biodiversity. Although the genetic bases of RI have been under intensive focus, many fundamental questions remain unanswered, including how many loci are needed to generate new species (4–6).

Two competing answers have been suggested in the speciation genetics literature. On the one hand, speciation may start when hybridization is strongly reduced by just a few genes with large effects on hybrid fitness (i.e., "master genes" of speciation), affecting key reproductive, behavioral, and ecological traits (7, 8). RI builds up faster when natural selection acts on a handful of speciation genes concentrated in few genomic regions (8–12), even more so if these are linked by reduced recombination as in inversions (13, 14). On the other hand, postzygotic isolation may be initiated gradually by multiple minor incompatibilities, such as Bateson–Dobzhansky–Muller interlocus epistatic incompatibilities that randomly accumulate across the entire genome as lineages diverge (15–17). After a certain point, the multiplying effects of this growing "mass of genes" erodes hybrid fitness (17–22). These two views imply different expectations regarding the relationship between RI and genetic divergence. Small-effect incompatibilities should gradually increase with divergence time (at least initially), while a few major-effect incompatibilities can be set off any time after divergence is initiated.

Another burning question in speciation genetics is whether sex chromosomes are hotspots for barrier loci, which in turn can illuminate on the evolutionary forces underlying hybrid incompatibilities (23). The role of sex chromosomes has been popularized by the two empirical "rules of speciation" (i.e., Haldane's rule and the large X-effect). Haldane's rule denotes that when a sex is absent, rare, or sterile in an interspecific cross, it is usually

Significance

Reproductive isolation is instrumental to the formation of new species (speciation), but it remains largely enigmatic how many incompatibilities are required to prevent hybridization and where they lie across the genome. By studying patterns of admixture in amphibian hybrid zones, we found that reproductive isolation is initiated by numerous small-effect incompatibilities scattered across the genome rather than concentrated in a few important genes. Unlike mammals and birds, in which Y/W degeneracy is a major cause of hybrid dysfunctions, the undifferentiated sex chromosomes of amphibians do not always host more genetic incompatibilities than other chromosomes. These combined results might explain why amphibian speciation is relatively slow, and its clock-like dynamics offer practical perspectives to categorize evolutionary lineages into species or subspecies.

Author contributions: C.D., M.V., N.P., and P.-A.C. designed research; C.D., A.B., D.L.J., G.M., T.S., D.C., A.N., L.F., S.D., I.M.-S., S.N.L., M.V., N.P., and P.-A.C. performed research; C.D., A.B., and D.L.J. analyzed data; and C.D. and P.-A.C. wrote the paper.

The authors declare no competing interest.

This article is a PNAS Direct Submission.

[1]To whom correspondence may be addressed. Email: Christophe.Dufresnes@hotmail.fr.

This article contains supporting information online at https://www.pnas.org/lookup/suppl/doi:10.1073/pnas.2103963118/-/DCSupplemental.

Published August 31, 2021.

the heterogametic sex (24), which has been verified in many animals (25). The large X-effect refers to the disproportionally high impact of X or Z chromosomes in driving hybrid dysfunctions compared to autosomes (26). Initially identified in *Drosophila* (4, 27), this rule has been verified by restricted introgression at sex-linked loci across many hybrid zones of mammals (28), birds (29), and insects (30).

It has become widely accepted that Haldane's rule and the large X-effect are primarily caused by hemizygosity on the X/Z chromosomes (due to the decayed nature of the Y/W), as they express recessive incompatibilities in the heterogametic sex (25, 31). Hence, one can predict that organisms whose gametologs have not degenerated, like most amphibians and fishes, should not follow these rules of speciation. Yet this prediction has rarely been explored empirically because of the difficulty of identifying morphologically similar (homomorphic) sex chromosomes (32, 33). Without the confounding effects of hemizygosity, the large X-effect then becomes an ad hoc test to assess the relative contribution of sex-linked genes in driving incompatibilities with alternative mechanisms (34), namely the faster evolution of male-expressed genes ("faster male" hypothesis, refs. 35–38) and of interacting X–Y genes necessary for the development of the heterogametic sex ("faster heterogametic sex" hypothesis, refs. 39, 40).

The genetic architecture of RI has been traditionally inferred from quantitative trait loci (QTL) mapping of incompatibilities segregating among hybrid progenies, as obtained from interspecies experimental crosses (4). This is only feasible in captive-bred organisms with a short generation time and, in practice, remains limited to a few laboratory model organisms (notably *Drosophila*). Furthermore, this approach lacks informativeness when RI is strongly polygenic, because genes of small individual effects are difficult to pinpoint. For less-accessible species, speciation researchers have screened for peaks of genome divergence between species pairs (41), which may be associated with RI (e.g., genes resisting introgression) and interspecies differentiation (e.g., genes evolving faster than the genome average). However, the landscape of divergence between closely related genomes does not depend only on their permeability to interspecific gene flow but also on intragenomic variation in recombination and mutation rates, which affects the level of background selection and thus diversity (42, 43). Direct approaches are therefore required to identify genomic regions that resist admixture because they harbor the genes involved in RI (6).

As an alternative to traditional speciation genetic studies, we addressed these fundamental questions by directly measuring the permeability of genetic barriers at various stages of divergence across natural species boundaries. We set up a multilevel comparative framework of hybrid zones between anuran amphibians from the Western Palearctic (WP), to test two key predictions of the master genes versus mass of genes views of speciation, and whether sex-linked loci are disproportionally involved without X/Z hemizygosity.

First, we explored the strength of RI with increased divergence by comparing patterns of introgression across 41 pairs of naturally hybridizing lineages, 15 of which could be analyzed by geographic cline analyses. We expected a monotonous relationship under the mass of genes hypothesis, as RI results from the cumulative effects of multiple mutations arising with the genetic divergence of lineages. Under the master genes hypothesis, however, RI should not increase regularly but might suddenly arise at any moment along the continuum of divergence.

Second, we examined the genomic landscape of introgression with locus-by-locus geographic cline analyses for a subset of nine transect-sampled hybrid zones targeted with restriction site–associated DNA–sequencing (RAD-seq) data. Under the master genes model, gene flow should first be drastically reduced at a few barrier loci and their surroundings (because of linked selection), while the rest of the genome still admixes more freely: Heterogeneous strengths of isolation among loci are thus expected when speciation starts. Under the mass of genes model, however, introgression should progressively decrease throughout the entire genome, as genetic divergence increases, until large parts entirely stop admixing: Heterogeneous levels of isolation are expected to appear later in the speciation process.

Finally, we exploited whole-genome assemblies available for the genera *Hyla* and *Rana*, as well as knowledge of their sex determination systems (44, 45), to test for large X-effects across their respective hybrid zones. Since these frogs feature homomophic sex chromosomes, large X-effects would indicate that hemizygosity is not the main driver of sex-linked incompatibilities.

Results

Geographic Patterns of Introgression. Analyses of the amount of RI between 41 hybridizing pairs of lineages, based on their phylogeographic transitions, support a general reduction of hybridizability as divergence increases (Fig. 1 and *SI Appendix*, Tables S1 and S2). This was the case when considering either divergence time or sequence divergence estimates at mitochondrial (16S, *cyt-b*, and COI) and nuclear markers (RAD-seq) (*SI Appendix*, Fig. S1)—which were all correlated (*SI Appendix*, Fig. S2).

The relationship was first suggested qualitatively by ranking the transitions into one of three categories of steepness (shallow, steep, and very steep). This allowed a comparison of the 41 pairs altogether, despite heterogeneity of sampling schemes that impeded quantifying the hybrid zone steepness in some of them (see *Methods*). The link was then confirmed quantitatively for a subset of 15 pairs in which hybrid zones could be thoroughly sampled along geographic transects and for which we could infer cline width (parameter w) from average population ancestry data (Fig. 1 and *SI Appendix*, Table S2).

Genomic Landscape of Introgression. For nine species pairs in which transect-sampled hybrid zones were analyzed with RAD-seq data, we fitted clines separately on hundreds/thousands of species-diagnostic SNPs (*SI Appendix*, Table S2). This revealed that the interlocus variation in introgression progressively decreases as the transitions become steeper (Figs. 2 and 3). The cline widths w were normally distributed around the genome average for the loosest hybrid zones, gradually shifted toward zero for intermediate transitions, until two modes emerged for the steepest transitions: loci that no longer introgress (w: ∼0) and loci that still do so (w: ∼10 to 20 km). Marker density in respect to genome size was variable between hybrid zones (∼10 to 1,488 species-diagnostic SNPs/gigabase) but was not associated to the proportion of steep clines retrieved (and thus the amount of putative barrier loci detected) (*SI Appendix*, Table S2). Because no genome assembly was available for most species pairs (see *Methods*), it was not possible to infer marker density in respect to the decay of linkage disequilibrium (LD) with physical distance along chromosomes.

For one species pair (*Hyla arborea*/*orientalis*), two replicate hybrid zones were analyzed in Serbia and Greece, with the same genetic markers for comparison. We recovered broadly similar distributions of cline widths w, which were correlated between the two transects (*SI Appendix*, Fig. S3), hence supporting the replicability of introgression patterns.

Large X-Effects. For four hybrid zones, RAD tags bearing species-diagnostic polymorphism were mapped to reference genomes. The homomorphic sex chromosomes of these species were previously identified (44, 45), allowing us to compare introgression between sex-linked and autosomal markers.

In *Rana temporaria*/*parvipalmata*, 419 SNPs with diagnostic alleles could be located on the thirteen linkage groups (LGs) of the *R. temporaria* genome: 91 sex linked (LG1) and 328 autosomal (LG2 to LG13). There was a significant effect of the LG

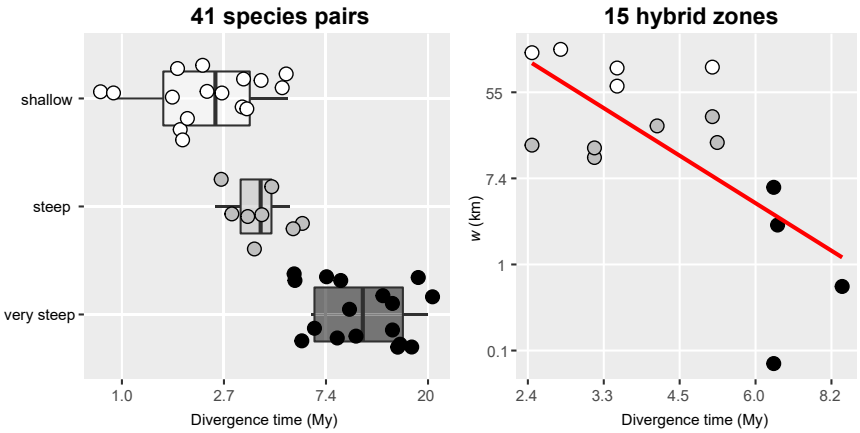

Fig. 1. Relationship between hybrid zone steepness and divergence time (log scaled). (*Left*) Inferred qualitatively from the phylogeographic transitions of 41 species pairs ranked in three categories (ordinal logistic regression; $P = 0.003$). Divergence significantly differed among categories (ANOVA, $F = 92.1$, $P = 1.1 \times 10^{-9}$, and $df = 1$) but without influence of the taxonomic group (genus) ($F = 0.85$, $P = 0.58$, and $df = 6$) nor their interaction ($F = 1.1$, $P = 0.39$, and $df = 9$). (*Right*) Inferred quantitatively from cline width w (log scaled) computed along transect-sampled hybrid zones of 15 species pairs (linear regression; $P = 0.004$, $R^2 = 0.48$, and $df = 13$).

(ANOVA, $F = 3.0$, $P = 4.5 \times 10^{-4}$, and $df = 12$), in which LG11 ($F = 6.9$, $P = 0.009$, and $df = 1$) and LG12 ($F = 16.9$, $P = 4.8 \times 10^{-5}$, and $df = 1$) both introgressed significantly less than the rest of the genome (Fig. 4). For the sex-linked LG1 loci, however, the width w was marginally higher compared to the autosomal loci ($F = 4.4$, $P = 0.04$, and $df = 1$; Fig. 5). Accordingly, LG1 did not stand out from the pairwise comparisons among LGs (Tukey tests; *SI Appendix*, Fig. S4), and there was no effect of sex linkage on w, based on an ad hoc permutation test ($P = 0.41$; *SI Appendix*, Fig. S5) (see *Methods*). More generally, the genomic landscape of w was homogenously variable across all chromosomes: Groups of loci with wide or narrow clines alternate over short genetic distances (Fig. 6).

In *Hyla i. intermedia*/*perrini*, 687 SNPs were mapped to the 12 LGs of *H. arborea*: 137 sex linked (LG1) and 550 autosomal (LG2 to LG12). There was a highly significant effect of the LG (ANOVA, $F = 8.9$, $P = 6.8 \times 10^{-15}$, and $df = 11$), in which only the sex-linked LG1 had a lower w than average ($F = 75.4$, $P < 2 \times 10^{-16}$, and $df = 1$, Figs. 4 and 5). This sex linkage effect stands out from the pairwise comparisons among LGs (Tukey test; *SI Appendix*, Fig. S4) and was confirmed by the ad hoc permutation test ($P < 0.001$; *SI Appendix*, Fig. S5).

In *H. arborea*/*orientalis*, 763 SNPs were mapped: 206 sex linked (LG1) and 557 autosomal (LG2 to LG12). In both transects, w substantially varied among LGs (ANOVA, $F = 12.7$, $P < 2 \times 10^{-16}$, and $df = 11$ in Serbia; $F = 9.0$, $P = 4.1 \times 10^{-15}$, and $df = 11$ in Greece; Fig. 4 and *SI Appendix*, Fig. S4), as several LGs introgressed less than the rest of the genome (i.e., LG1 [$F = 44.8$, $P = 4.2 \times 10^{-11}$, and $df = 1$] and LG6 [$F = 11.1$, $P = 9.0 \times 10^{-4}$, and df = 1] in Serbia and LG1 [$F = 24.7$, $P = 8.3 \times 10^{-7}$, and df = 1] and LG08 [$F = 14.8$, $P = 1.3 \times 10^{-4}$, and $df = 1$] in Greece). Taking each transect separately, the effect of sex linkage did not reach significance in the permutation tests ($P = 0.26$ for Greece and $P = 0.12$ for Serbia; *SI Appendix*, Fig. S5). However, LG1 was the only LG to introgress less than average in both transects (and had the lowest P in both) (see also pairwise Tukey tests; *SI Appendix*, Fig. S4). Combining the two datasets, and considering locus and transects as additional random variables, the analysis thus clearly highlighted a sex linkage effect in this species pair as well ($P < 0.001$; *SI Appendix*, Fig. S5).

Discussion

Speciation by a Mass of Genes in Amphibians. Our comparative framework of hybrid zones provides two lines of evidence in support of the mass of genes hypothesis for the buildup of postzygotic isolation in frogs and toads of the WP region. Firstly, the geographic extent of introgression regularly decreases as the genetic divergence increases (Fig. 1). This tendency is supported by a fairly large number of species pairs representative of many families and thus appears generalizable at least to WP anurans. Here, the link holds true for the several divergence estimates tested (*SI Appendix*, Fig. S1) and whether we considered all species pairs in extensive (but less accurate) qualitative comparisons or only transect-sampled hybrid zones in more accurate (but less extensive) quantitative comparisons (Fig. 1). Moreover, potential events of past introgression should have negligible effects on our results, since we incorporated divergence time and genetic distances measured from mitochondrial phylogenies, or nuclear phylogenies based on pure populations far away from the present contacts (*SI Appendix*, Table S1). The seemingly clock-like reduction of hybridizability with divergence suggests a polygenic origin of the incompatibilities (i.e., multiple barrier loci cumulating their effects) rather than just a few major ones—which could have otherwise emerged at any moment along the continuum of divergence. Secondly, the late accumulation of hundreds of barrier loci is directly visible from our locus-by-locus cline analyses: RI starts by lowering the width of the clines homogenously across chromosomes when RI is weak (given the large hybrid zones) before a fraction of loci become impermeable to gene flow when RI is clearly stronger (given the narrower hybrid zones) (Figs. 2 and 3). For the *R. temporaria*/*parvipalmata* hybrid zone, where we benefited from a genome assembly, the homogeneous genomic landscape of introgression confirms that RI implicates numerous loci that are not constrained to particular genomic regions (Fig. 6). The relationship between hybridizability and divergence is reminiscent of experimental results in various plant and animal groups (3), including W. F. Blair's classical hybrid inviability data in anurans (46). Here, our study is quite complementary, as the degree of RI and its genomic architecture were inferred from currently admixing natural populations, hence allowing to consider both extrinsic and intrinsic postzygotic isolation.

If RI in WP anurans is initiated by the additive effects of numerous weak genetic incompatibilities, it is reasonable to assume that postzygotic isolation is the main driver of speciation. Consistently, most of our focal lineages are "cryptic" (i.e., they exhibit no obvious morphological, acoustic, or behavioral differences potentially responsible for premating and/or extrinsic postzygotic barriers). This assumption remains to be thoroughly tested, however, especially at the chemical level (e.g., pheromones),

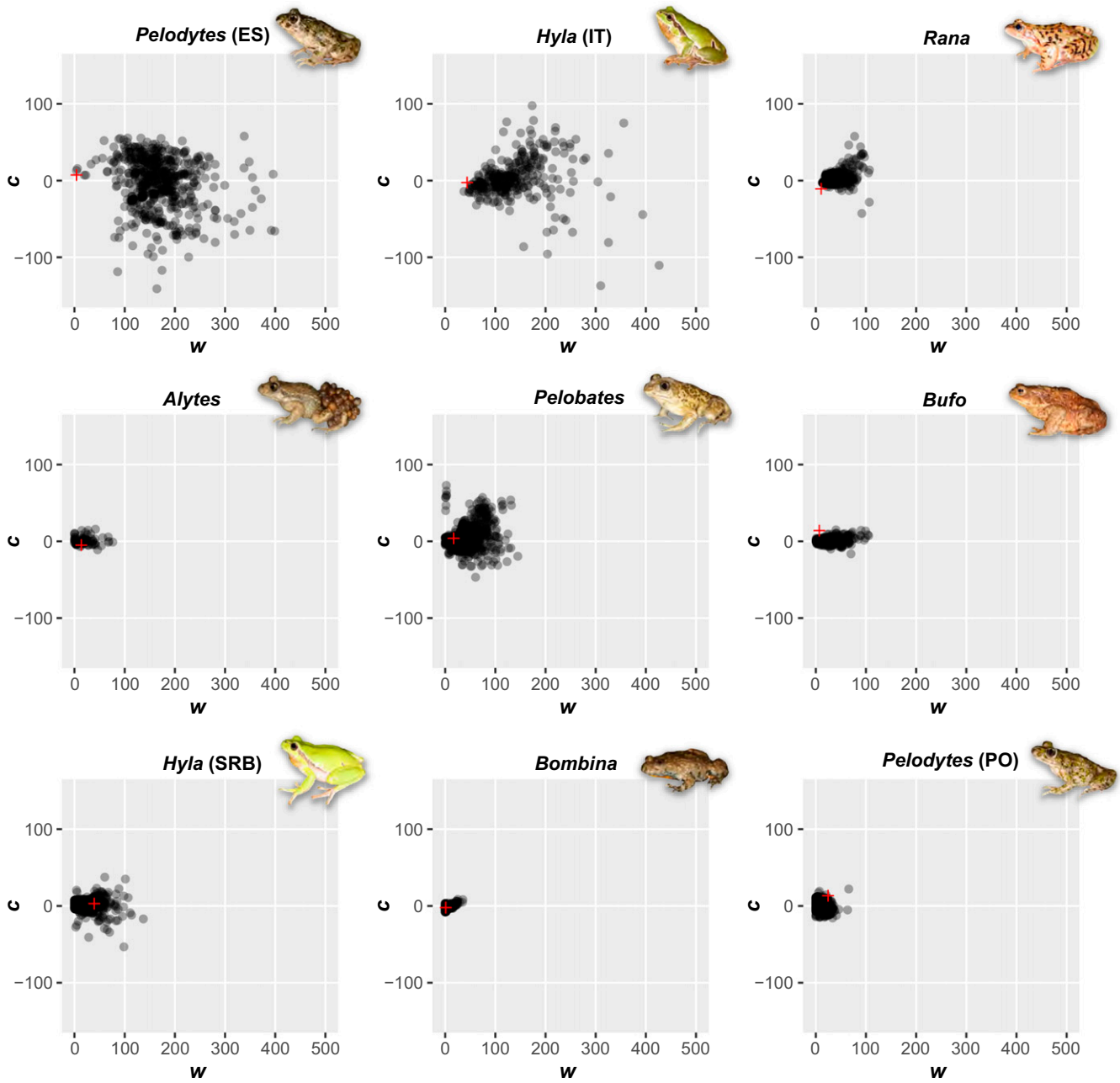

Fig. 2. Variation in cline center *c* and width *w* in WP anuran hybrid zones. Cline parameters (in kilometers) were estimated for lineage-diagnostic SNPs genotyped across transects for nine hybrid zones representative of the speciation continuum, arranged by the median of *w* (*SI Appendix*, Table S2): *P. p. punctatus/hespericus* in Spain (ES); *H. i. intermedia/perrini* in Italy (IT); *R. temporaria/parvipalmata*; *Alytes obstetricans/almogavarii*; *Pelobates fuscus/vespertinus*; *Bufo bufo/spinosus*; *H. arborea/orientalis* in Serbia (SRB); *Bombina bombina/variegata*; *Pelodytes atlanticus/ibericus* in Portugal (PO). Each black dot is a SNP locus; the red crosses show the mitochondrial clines. The center *c* is given as the deviation from the median center. Photograph credits: C.D.

which potentially play important roles in amphibians, including anurans (47). In the absence of direct assessments (e.g., mate choice experiments), the composition of genotypes in the center of the contact zones can offer clues on the strength of extrinsic barriers: Bimodal or trimodal hybrid zones indicate a deficit of hybrids, resulting either from their low fitness or from low rates of interspecific crossing. Although our sampling does not include populations from the hybrid zone center in all cases, the ones available feature unimodal distributions of the hybrid index, hence random mating (e.g., *Bombina*, *Rana*, and *Pelodytes*; *SI Appendix*, Table S2 and references therein). Moreover, because fertilization is external in frogs, anatomical prezygotic incompatibilities are not expected, and sexual selection is potentially less efficient compared to other groups such as insects or birds. In WP anurans, we thus hypothesize that speciation is primarily initiated by intrinsic postzygotic isolation caused by a mass of minor genetic incompatibilities, which restrain interspecific gene flow but do not trigger prezygotic isolation.

Under this hypothesis, mechanisms that reduce crossbreeding—such as bioacoustic differentiation—will essentially evolve during later stages of divergence, perhaps via reinforcement (48, 49). In our focal groups, all the young cryptic lineages accordingly feature alloparapatric distributions because, without premating barriers,

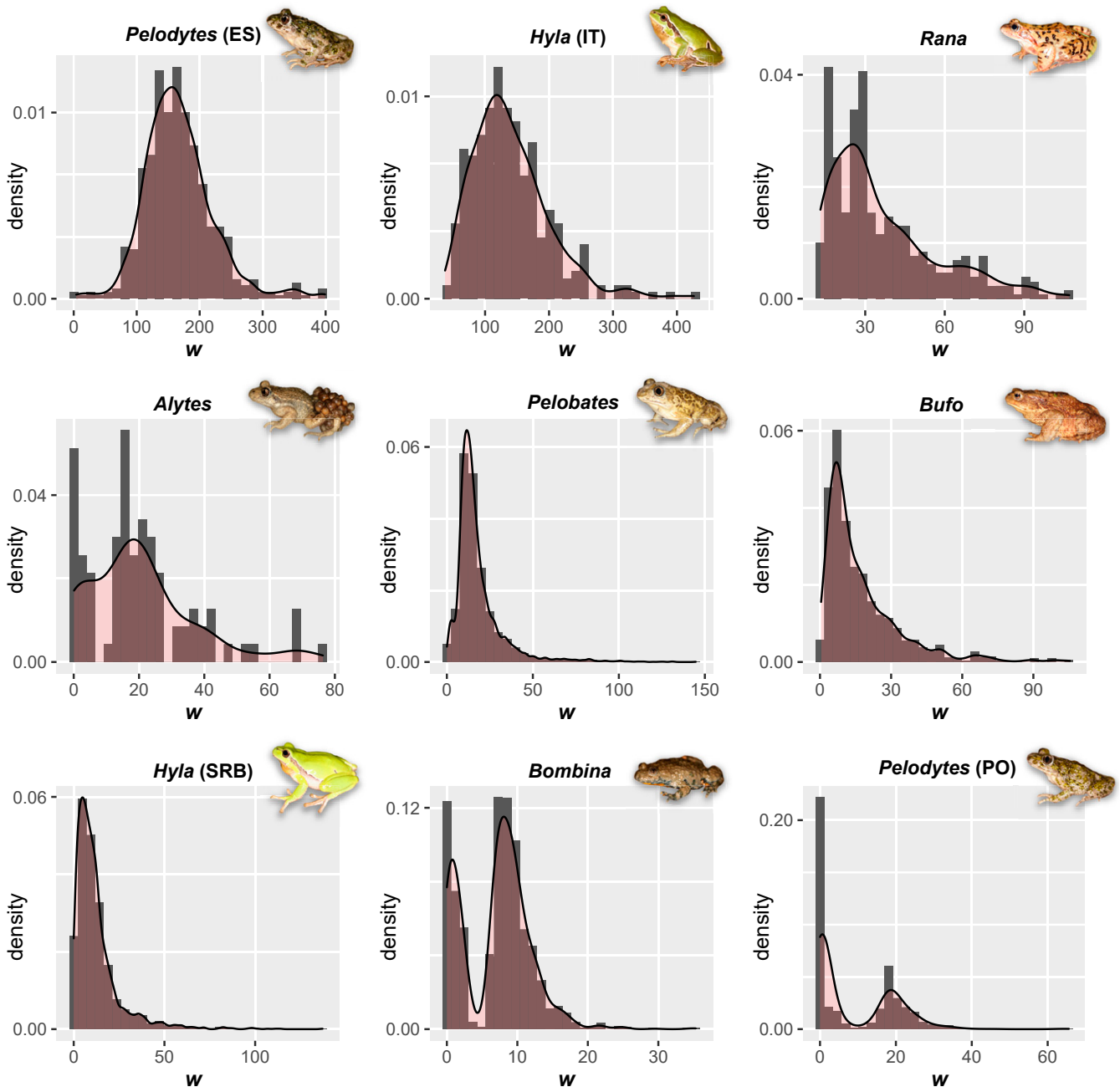

Fig. 3. Distribution of cline width *w* in WP anuran hybrid zones. *w* (in kilometers) was estimated for lineage-diagnostic SNPs genotyped across transects between nine pairs of anuran taxa representative of the speciation continuum, arranged by the median of *w* (*SI Appendix*, Table S2; lineages detailed in the legend of Fig. 2). For each, a density function is overlain over the empirical data, illustrating how *w* progressively abuts zero throughout the genome, spanning from a unimodal distribution (*Pelodytes* [ES] and *Hyla* [IT]) to a Poisson distribution (*Rana*, *Alytes*, *Pelobates*, *Bufo*, and *Hyla* [SRB]) and a bimodal distribution (*Bombina* and *Pelodytes* [PO]). Notice that the scales of the *x*-axes are adjusted for each case. Photograph credits: C.D.

introgressive hybridization precludes the emergence of sympatry. Consequently, only the most diverged, phenotypically distinct species can share overlapping distributions and habitats, and admixture is no longer observed: if produced, hybrids are unfit (e.g., *H. arborea*/*meridionalis*, ref. 50) or propagate via alternative modes of reproduction such as allopolyploidy (e.g., *Bufotes*, ref. 51) or hybridogenesis (e.g., *Pelophylax*, ref. 52).

While genetic incompatibilities seem to be the initial driver of speciation in WP anurans, this is not necessarily the case for other animal groups or biomes. The extensive study of the mechanisms of RI in birds has led some authors to suggest a major role for mate choice, via both pre- and postzygotic mechanisms (53–55). In birds, sympatry is sometimes achieved before the evolution of substantial genetic incompatibilities, and gene flow between closely related species often remains pervasive for a long time (56), except at loci involved in key phenotypes facing divergent selection. For instance, plumage coloration genes can stabilize avian hybrid zones (57). Nevertheless, single genes are rarely enough to guarantee advanced ecological or behavioral isolation, and emerging genomic data suggests that even rapid speciation, as in adaptive radiations, is driven by multiple genomic regions, especially when the traits involved are polygenic (e.g., cichlids, ref.

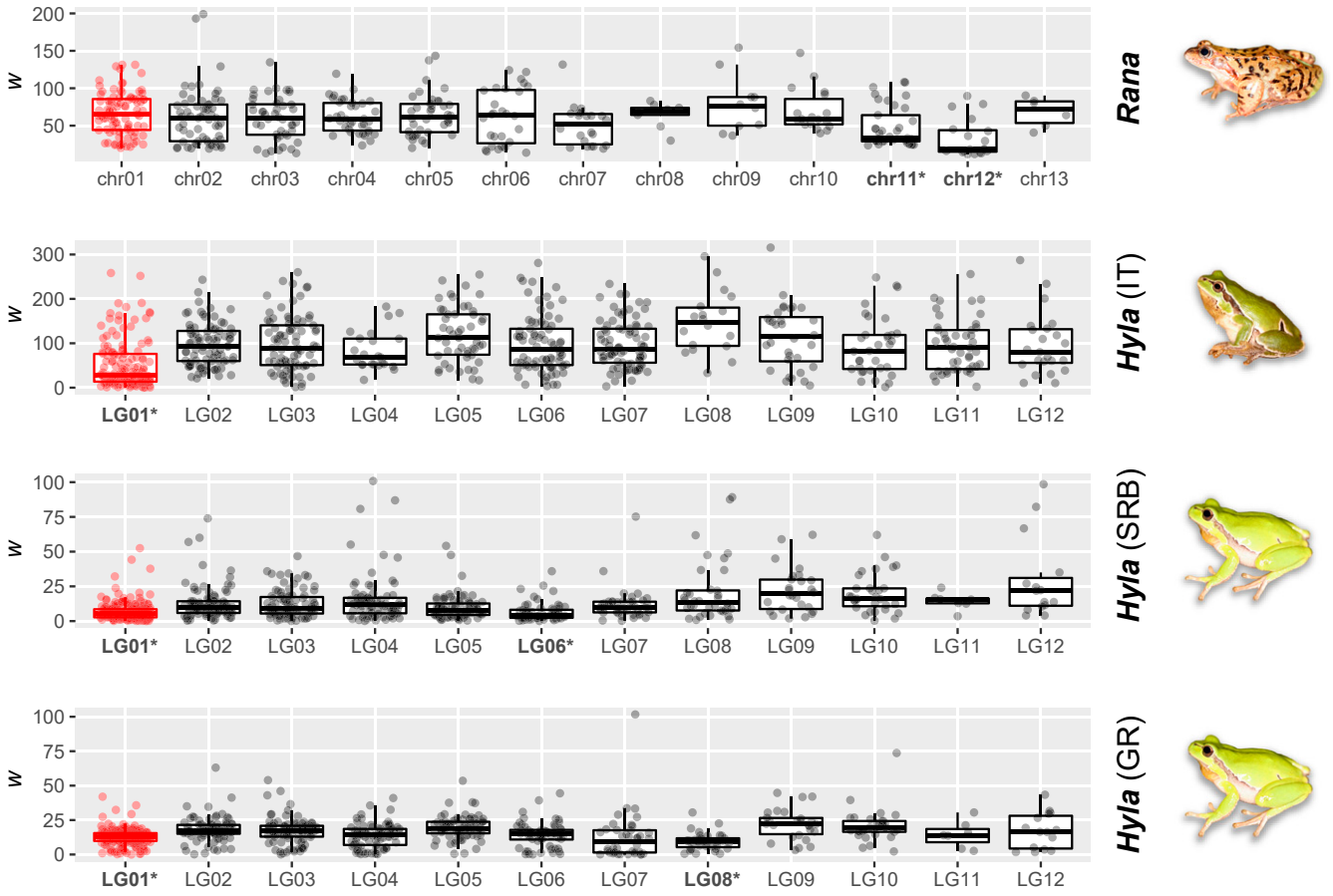

Fig. 4. Cline width *w* per LGs in WP anuran hybrid zones. Estimates are in kilometers. LG1/chr01 bears the sex-determining locus (in red). From top to bottom are the following: *R. temporaria*/*parvipalmata* in northern Spain, *H. i. intermedia*/*perrini* in Italy (IT), and *Hyla arborea*/*orientalis* in Serbia (SRB) and Greece (GR). An LG effect on *w* was evidenced for all systems, and the LGs contributing to the effect with a significantly lower *w* than the rest of the genome are highlighted in bold and asterisks (see *Results* for statistical details). Photograph credits: C.D.

58). The general mode of RI should then affect speciation rates: Evolving RI via genetic divergence distributed throughout the genome (as in anurans) should take longer than via behavioral or ecological isolation relying on a simple or even polygenic architecture (as e.g., in birds and cichlids). Accordingly, prezygotic barriers often reach completion faster than intrinsic postzygotic barriers (59, 60). Here, this hypothesis is consistent with the overall slow speciation clock of amphibians compared to other vertebrate classes (61, 62) and particularly birds [~5.3 My versus 1.2 My (62)].

The crucial role of intrinsic incompatibilities in driving speciation was recognized early on (24, 63–65) but has more recently been shadowed by the rising idea that even weakly diverged and compatible lineages could represent distinct species (i.e., if hybridization diminishes early in the process) because of ecological and behavioral constraints (66, 67). This perception is biased by the disproportionally large amount of speciation research focused on ecological speciation, in which adaptation is directly responsible for isolation (68). A more balanced view on the respective importance of genetic versus behavioral/ecological isolation in animals will require comparisons spanning multiple clades and biomes. We suggest that the trend followed by WP anurans—in which genetic divergence first generates intrinsic isolation in alloparapatry before behavioral isolation evolves and allows sympatry—might happen more frequently than the recent speciation literature implies.

What Role for Homomorphic Sex Chromosomes? In anuran amphibians, which bear undifferentiated sex chromosomes (69), the large X-effect has received little support. We showed no effect in *Rana* (Figs. 4 and 5), as previously suggested for *Bufotes* (70). Hybrid incompatibilities also predominantly map to autosomes in *Xenopus* frogs (32). This implies little role for sex-linked genes without hemizygosity. One reason could be the lack of specialization of the young anuran sex chromosomes (71), which are frequently recycled by turnovers (44) and/or are maintained undifferentiated by recombination (72). As a consequence, they do not necessarily attract genes with sex-antagonistic functions (71), which could in turn act as barrier loci by causing faster male or faster heterogametic sex incompatibilities. Here, this is well-illustrated by our *Rana* hybrid zone, where the sex-determining region did not show particularly reduced introgression (Fig. 6). Beyond frogs, only few organisms with homomorphic sex chromosomes have been studied in a speciation context, and large X-effects were also not recovered (e.g., poplars, ref. 73).

Tree frogs (*Hyla*) seem to make an exception. There was a significant large X-effect for the pair *H. i. intermedia*/*perrini* and a trend for the pair *H. arborea*/*orientalis*, as previously suggested (33). Either their Y chromosome did accumulate genes with male-specific functions—intrinsically reducing hybrid fitness by faster male or faster heterogametic sex mechanisms—or it possibly exhibits some hemizygosity. Sex chromosomes are clearly homomorphic in most hylids (74) but nascent X–Y differentiation was documented across the species investigated here, potentially because of recent recombination arrests (75).

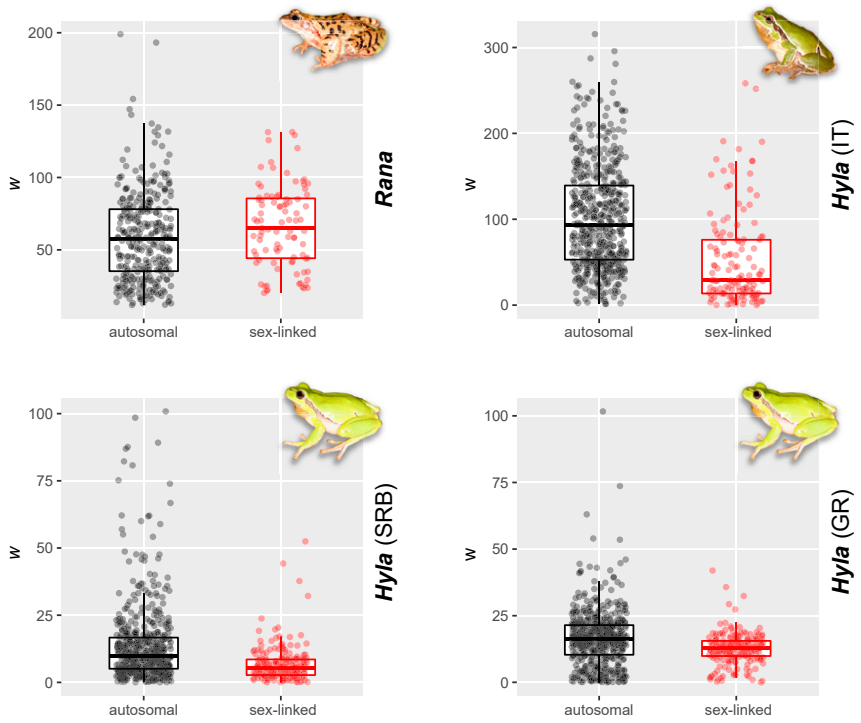

Fig. 5. Cline widths *w* for autosomal (black) and sex-linked loci (red) in WP anuran hybrid zones. Estimates are in kilometers. From top left to bottom right are the following: *R. temporaria*/*parvipalmata* in northern Spain, *H. i. intermedia*/*perrini* in Italy (IT), *H. arborea*/*orientalis* in Serbia (SRB) and in Greece (GR). No large X-effect was found in *Rana*, where LG1 even admixes slightly more than the rest of the genome (see also Fig. 4). A large X-effect is evident in the Italian *Hyla* hybrid zone, where LG1 (the sex chromosomes) is the only LG to significantly introgress less than the rest of the genome. In *H. arborea*/*orientalis*, LG1 is not the only LG to significantly introgress less in the Serbian (*Left*) and Greek (*Right*), transects, but it is the only one to do it in both (Fig. 4), thus also suggesting a large X-effect. Photograph credits: C.D.

If homomorphic sex chromosomes do not play a disproportionate role in the buildup of RI (as in *Rana*, *Bufotes*, and *Xenopus*)—unless some X–Y divergence has been initiated (as perhaps in *Hyla*)—this would indirectly suggest that hemizygosity must account for most of the large X- or Z-effects documented in organisms with decayed gametologs (as in mammals, birds, and *Drosophila*). Accordingly, RI builds faster in species bearing heteromorphic compared to homomorphic sex chromosomes (76, 77). In addition to the mode of RI (see *Speciation by a Mass of Genes in Amphibians*), the lack of sex chromosome differentiation could thus further contribute to the slow pace of amphibian speciation. More in-depth insights could also be gained from comparing XY versus ZW species, in which faster male and faster heterogametic sex mechanisms imply different assumptions regarding Haldane's rule and the large X-effect (25, 32). Both of these key aspects of speciation obviously deserve further exploration prior to make generalizations on the role of homomorphic sex chromosomes. Large X-effects have been tested in very few amphibian models so far (now six), because of the methodological challenges of identifying their sex determination systems and mapping species-diagnostic loci to compare sex-linked versus autosomal patterns of introgression. In parallel, Haldane's rule certainly needs reevaluation in anurans. Previous assessments assumed conserved patterns of heterogamety among major clades (46), yet it has recently been shown that heterogametic switches occurred even between closely related species (45, 78).

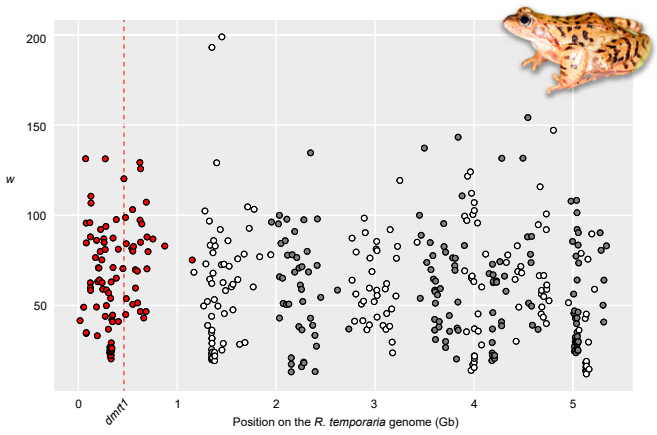

Fig. 6. Genomic landscape of cline widths *w* across the *R. temporaria*/*parvipalmata* hybrid zone. Estimates are in kilometers for 419 species-diagnostic SNPs mapped on the *R. temporaria* genome. Colors distinguish adjacent chromosomes. The sex chromosome pair (LG1) is in red, and the position of the sex-determining gene *dmrt1* is highlighted. Loci showing reduced introgression are homogeneously distributed throughout the genome. Photograph credit: C.D.

Implications for the Delimitation of Incipient Species. In systematics, if one accepts a ranked system in which strongly isolated and freely introgressing lineages should be afforded species and subspecies ranks, respectively (79–81), the difficulty is to translate the continuous progress of RI into a dichotomous classification, i.e., where to cut through the "grey zone" of speciation (82). When lineages meet, the structure of their hybrid zones can be used (83). Strong LD in hybrids reflects little mixing between the parental genomes, which is clearly indicative of advanced RI and thus distinct species (84, 85). Parapatric transitions in which admixture decreases LD are harder to categorize. Narrow hybrid

zones maintained by selection represent stable reproductive boundaries (83), and the taxa involved should thus also be treated as species. However, in many cases, it is difficult to assess whether introgression reflects neutral diffusion or selective barriers.

We suggest here that for such unimodal hybrid zones, practical guidelines can be derived from the architecture of introgression. There is a tipping point in the speciation process beyond which the lineages will never merge back: It is reached once the mass of incompatibilities cumulates, shaping the multilocus clines toward null widths (Figs. 2 and 3). Hence, we propose to assign the species rank when the cline widths shift toward a Poisson or a bimodal distribution abutting zero—the cue that many markers are putatively linked to barrier loci (Fig. 3). In contrast, if the widths essentially follow a Gaussian distribution, the interacting taxa may rather be considered as incompletely separated lineages or subspecies (79–81). Applying these principles here, the hybrid zones *P. p. punctatus*/*hespericus* in Spain and *H. i. intermedia*/*perrini* in Italy would feature conspecific lineages, while the remaining seven transitions would reflect species-level lineages (Figs. 2 and 3). Furthermore, given that the interlocus variation of cline estimates proportionally decreases with the genome average width, the latter could even be used as proxy: A large proportion of sharp clines emerge for all our hybrid pairs once the average cline falls below 30 km (e.g., last seven panels in Figs. 2 and 3). The actual strength of RI reflected by geographic clines obviously depends on dispersal across the hybrid zones, so the decisive threshold of cline width should ideally be calibrated for each species group. While interlocus variation of w has the advantage of being independent from dispersal (for autosomal loci), the approach will be limited for taxa with patchy distributions, since the fraction of loci with null widths shall depend on the density of sampling near the hybrid zone center. Still, the pattern highlighted here can serve as baseline for molecular taxonomy under integrative views of the biological species criterion (79–81, 86–89).

One drawback of this approach is the need for geographic contacts in order to assess introgression between candidate lineages. Fortunately, our results also provide some thresholds for ranking allopatric taxa. In European anurans, lineages that evolved ≥6 My and show ≥0.4% divergence at RAD sequences (obtained by our procedures) or ≥3% at 16S sequences invariably form narrow transitions. Below 2 My and 0.3% of RAD divergence, the hybrid zones are almost exclusively shallow (Fig. 7). These yardsticks can thus be used in a preliminary categorization of taxa following the "hybrid zone approach" (86, 90), even without actual hybrid zone data. Case by case assessments will remain necessary for the situations in between, for which the outcomes of secondary contacts can greatly vary, even among the same species pairs (91). Pending some knowledge of the speciation clock, the principle can be generalized to any organismal group, as long as RI follows the mass of genes model. If, however, speciation is driven by the master genes model or relies on behavioral cues (e.g., birds), it might then be more relevant to quantify and categorize divergence in the signals themselves (92). By combining assessments of both phylogenetic independence and restricted gene flow at secondary contact, our approach will hopefully find some consensus among researchers adopting either the lineage or biological definition of species, and ultimately limit questionable taxonomic inflation.

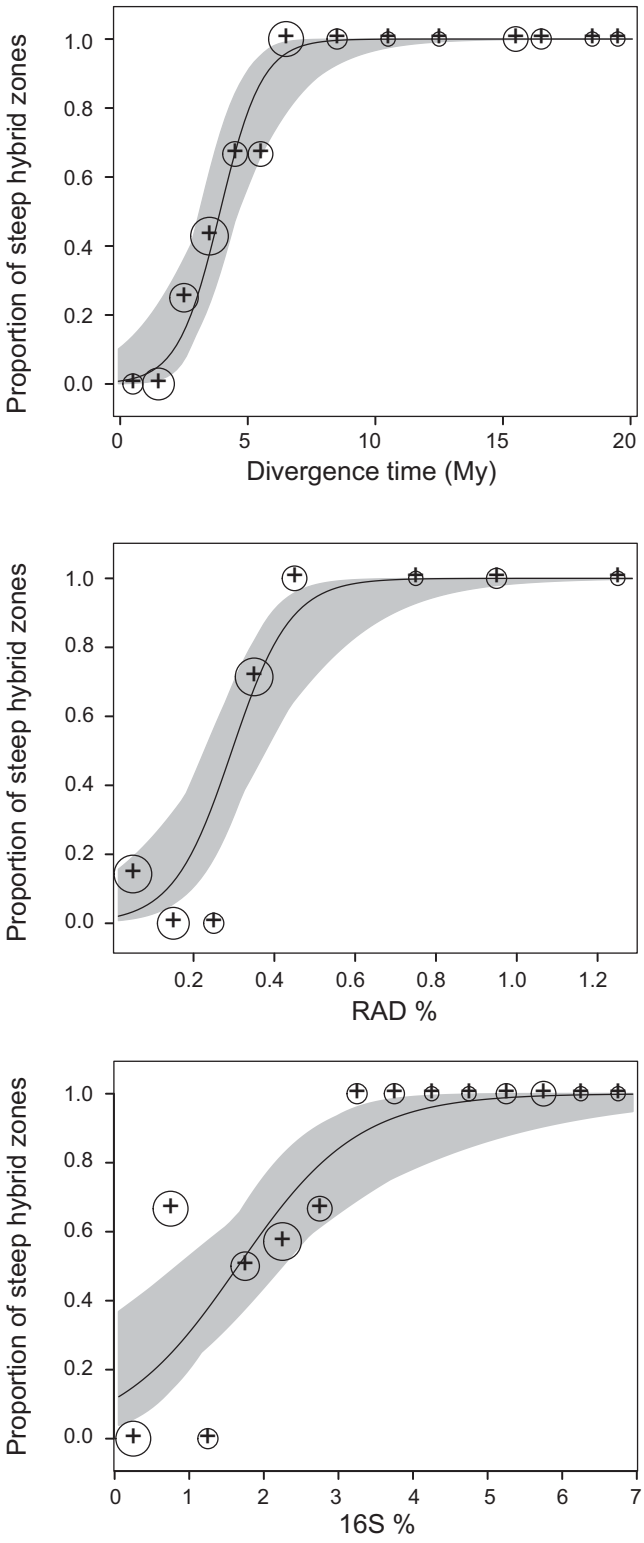

Fig. 7. Probability to speciate in relation to divergence. Graphs show the proportion of steep hybrid zones in respect to divergence time (*Top*, 1 My windows), percent of RAD sequence divergence (*Middle*, 0.1% windows), and percent of 16S divergence (*Bottom*, 0.5% windows). The empirical data are shown in crosses, with circles being proportional to the number of tested lineage pairs. The lines and gray areas are sigmoid clines fitted by maximum-likelihood to this data (and its 95% CI). Equal probabilities to form steep or shallow hybrid zones are reached by 3.3 My, 0.3% of RAD divergence and 1.7% of 16S divergence.

Methods

Study Systems. We compared the extent of admixture across 41 pairs of WP anuran lineages based on multilocus nuclear analyses (introns, microsatellites, allozymes, and/or RAD-seq) and independently documented by our own previous phylogeographic studies. This encompassed painted frogs (*Discoglossus*, two pairs), midwife toads (*Alytes*, three pairs), fire-bellied toads (*Bombina*, one pair), spadefoot toads (*Pelobates*, six pairs), parsley frogs (*Pelodytes*, three pairs), tree frogs (*Hyla*, eight pairs), green toads

(*Bufotes*, eight pairs), common toads (*Bufo*, one pair), brown frogs (*Rana*, one pair), and water frogs (*Pelophylax*, eight pairs). Sources and summaries of the patterns of hybridization are reported in *SI Appendix*, Table S1.

When available, we harvested sequences from commonly used mitochondrial (*16S*, *cyt-b*, and COI) and nuclear (RAD-seq) markers for each pair of lineages to measure their percent of sequence divergence (MEGA X, ref. 93). We also incorporated divergence time estimates obtained from time-calibrated phylogenies (*SI Appendix*, Table S1).

While some transitions were collected along predesigned transects, sampling in others was more geographically scattered. In an effort to cover a maximum number of transitions but accounting for the variability of sampling schemes, we first categorized the transition of each species pair as either 1) shallow, with widespread introgression (>50 km from the contact); 2) steep, with moderate introgression (10 to 50 km around the contact); and 3) very steep, with occasional hybridization without introgression or weak introgression restricted to the immediate vicinity of the contact (<10 km) (*SI Appendix*, Table S1). The effect of divergence was tested in two ways: 1) by an ordinal logistic regression, considering the three categories as factors and 2) by two-way ANOVAs, in which the effect of the taxonomic group (= genus) was also considered.

Transition Widths. For a subset of 15 species pairs in which transitions were specifically sampled along transects, we quantified the geographic extent of admixture by fitting clines on the average nuclear ancestries of populations (*SI Appendix*, Table S2). The allele frequency of parental species should decrease from one gene pool to the other in a clinal manner, as a result of dispersal and selection against hybrids. The transition was modeled as a cline determined by its center *c* and width *w*, which correspond to the location and steepness of the transition, respectively. Steep transitions may further feature weak but geographically extensive introgression far from the center, following the diffusion of neutral alleles. In such cases, exponential tails flanking the cline may increase the fit on the empirical data, albeit with the cost of additional parameters (two for each tail). Clines were fitted with the maximum-likelihood algorithm of *hzar* (94) on population ancestry data (hybrid index) obtained from multilocus clustering analyses (*SI Appendix*, Table S2). We estimated the likelihood of each cline model (with or without exponential tails) and reported the one with the lowest Akaike information criterion value. The relationship between the genome average width and divergence time was assessed by a linear regression on log-transformed data.

Within-Genome Variation of Introgression. To assess the heterogeneity of introgression throughout the genome, we analyzed RAD-seq data from hybrid zones between nine pairs of lineages chosen to broadly cover the speciation continuum, i.e., admixing across very short (<10 km) to very large (>100 km) distances (*SI Appendix*, Table S2). All datasets were generated from genomic libraries prepared with a double-digest RAD-seq protocol (95), sequenced using an Illumina HiSeq 2500 (single read 125) and bioinformatically processed (demultiplexing and SNP calling) via the Stacks pipeline. Eight datasets were produced from the raw sequencing data of our previous work on *Alytes* (one pair), *Bombina* (one pair), *Hyla* (one pair), *Bufo* (one pair), *Pelobates* (one pair), *Rana* (one pair), and *Pelodytes* (two pairs) (96). Using the same procedures, a ninth dataset was produced from newly generated RAD-seq data for two independent hybrid zones between *H. arborea* and *H. orientalis* in northeastern Greece and northeastern Serbia (ref. 96, samples from ref. 33), allowing us to compare introgression patterns between replicate transects of the same species pair. The sources and details of each dataset are provided in *SI Appendix*, Table S2.

For each dataset, species-diagnostic SNPs were selected as those with fixed (frequency difference of 1.0) or nearly fixed alleles (frequency difference of >0.8) between the edge populations, and cline analyses were performed on the allele frequencies separately for each locus with *hzar*.

Large X-Effects. Testing for the role of sex chromosomes as hotspots for barrier loci has two prerequisites: 1) a genome assembly with scaffolds assigned to chromosomes or LGs, on which to align the species-diagnostic SNPs sequenced in the hybrid zone samples, and 2) knowledge of which LG harbors the sex-determining locus in the species pairs involved. These requirements were met for *Rana* and *Hyla*, for which the available RAD-seq data span four hybrid zones. In *Rana*, we aligned the loci genotyped in the *R. temporaria/parvipalmata* hybrid zone on a PacBio genome assembly of *R. temporaria* (available here: https://github.com/DanJeffries/Rana-temporaria-genome-assembly/), anchored by high-density linkage maps following ref. 44. For *Hyla*, we mapped the loci genotyped in the *H. i. intermedia/perrini* transition and the two *H. arborea/orientalis* transects on an unassembled, low-coverage draft genome of *H. arborea* (DOI: 10.5061/dryad.n856c) also anchored by a high-density linkage map (95). In all these lineages, sex is known to be determined by male heterogamety (XY) at LG1 (44, 45). Clines were analyzed for aligned loci that showed frequency differences above 0.7 between the parental populations.

Large X-effects should be reflected by narrower widths *w* for LG1 compared to autosomal LGs. In each hybrid zone, we assessed whether *w* significantly varied among LGs by ANOVA. Post hoc pairwise Tukey's tests were then applied to identify which LGs significantly introgressed less than the genome average. To further assess whether sex linkage influenced the amount of introgression, we designed a permutation test in which the assignment of each locus to an LG, and the assignment of each LG as the sex chromosomes, was shuffled 1,000 times. Each time, the effect of sex linkage on *w* was estimated in generalized linear mixed models, considering LG as a random factor, and the test statistic was recorded. The test statistic from the empirical data was then plotted against this null distribution and was considered significant if it fell above the 95% quantile. For *H. arborea/orientalis*, we also performed the analysis by pooling the data from the two transects together, considering transect and loci (the two transects were genotyped for the same loci) as additional random factors.

Data Availability. Raw sequence reads obtained by RAD-seq have been deposited in National Center for Biotechnology Information Sequence Read Archive, and are available under Bioproject PRJNA542138. All other study data are included in the article and/or *SI Appendix*.

ACKNOWLEDGMENTS. Thanks must go to our numerous collaborators who contributed to the phylogeographic datasets analyzed in this study. We are also grateful to R. Butlin for support. This study was funded by the Swiss NSF (Grant No. 31003A_166323 to N.P. and Fellowship No. P2LAP3_171818 to C.D.) and the Russian Foundation for Basic Research (Grant No. 20-04-00918 to S.N.L.). C.D. and M.V. were further supported by the Taxon-Omics priority program (SPP1991) of the Deutsche Forschungsgemeinschaft (Grant No. VE247/19-1).

1. P. Nosil, J. Feder, S. M. Flaxman, Z. Gompert, Tipping points in the dynamics of speciation. *Nat. Ecol. Evol.* **1**, 0001 (2017).
2. J. Kulmuni, R. K. Butlin, K. Lucek, V. Savolainen, A. M. Westram, Towards the completion of speciation: The evolution of reproductive isolation beyond the first barriers. *Philos. Trans. R. Soc. B* **375**, 20190528 (2020).
3. J. M. Coughlan, D. R. Matute. The importance of intrinsic postzygotic barriers throughout the speciation process. *Philos. Trans. R. Soc. B* **375**, 20190533 (2020).
4. J. A. Coyne, H. A. Orr, *Speciation* (Sinauer Associates, Sunderland, MA, 2004).
5. J. B. W. Wolf, J. Lindell, N. Backström, Speciation genetics: Current status and evolving approaches. *Philos. Trans. R. Soc. Lond. B Biol. Sci.* **365**, 1717–1733 (2010).
6. P. Nosil, J. L. Feder, Z. Gompert, How many genetic changes create new species? *Science* **371**, 777–779 (2021).
7. M. R. Servedio, G. S. Van Doorn, M. Kopp, A. M. Frame, P. Nosil, Magic traits in speciation: 'Magic' but not rare? *Trends Ecol. Evol.* **26**, 389–397 (2011).
8. S. M. Flaxman, A. C. Wacholder, J. L. Feder, P. Nosil, Theoretical models of the influence of genomic architecture on the dynamics of speciation. *Mol. Ecol.* **23**, 4074–4088 (2014).
9. R. Ueshima, T. Asami, Evolution: Single-gene speciation by left-right reversal. *Nature* **425**, 679 (2003).
10. H. A. Orr, The genetic basis of reproductive isolation: Insights from *Drosophila*. *Proc. Natl. Acad. Sci. U.S.A.* **102** (suppl. 1), 6522–6526 (2005).
11. D. C. Presgraves, Speciation genetics: Epistasis, conflict and the origin of species. *Curr. Biol.* **17**, R125–R127 (2007).
12. P. Nosil, D. Schluter, The genes underlying the process of speciation. *Trends Ecol. Evol.* **26**, 160–167 (2011).
13. L. H. Rieseberg, Chromosomal rearrangements and speciation. *Trends Ecol. Evol.* **16**, 351–358 (2001).
14. P. Jay *et al*., Supergene evolution triggered by the introgression of a chromosomal inversion. *Curr. Biol.* **28**, 1839–1845.e3 (2018).
15. J. H. Muller, *The New Systematics*, J. S. Huxley, Ed. (Clarendon, Oxford, 1940).
16. M. Turelli, H. A. Orr, The dominance theory of Haldane's rule. *Genetics* **140**, 389–402 (1995).
17. H. A. Orr, M. Turelli, The evolution of postzygotic isolation: Accumulating Dobzhansky-Muller incompatibilities. *Evolution* **55**, 1085–1094 (2001).
18. H. A. Orr, The population genetics of speciation: The evolution of hybrid incompatibilities. *Genetics* **139**, 1805–1813 (1995).
19. T. C. Mendelson, B. D. Inouye, M. D. Rausher, Quantifying patterns in the evolution of reproductive isolation. *Evolution* **58**, 1424–1433 (2004).
20. S. Gourbière, J. Mallet, Are species real? The shape of the species boundary with exponential failure, reinforcement, and the "missing snowball." *Evolution* **64**, 1–24 (2010).
21. D. R. Matute, I. A. Butler, D. A. Turissini, J. A. Coyne, A test of the snowball theory for the rate of evolution of hybrid incompatibilities. *Science* **329**, 1518–1521 (2010).
22. L. C. Moyle, T. Nakazato, Hybrid incompatibility "snowballs" between *Solanum* species. *Science* **329**, 1521–1523 (2010).

23. K. K. Lund-Hansen, C. Olito, E. H. Morrow, J. K. Abbott, Sexually antagonistic coevolution between the sex chromosomes of *Drosophila melanogaster*. *Proc. Natl. Acad. Sci. U.S.A.* **118**, e2003359118 (2021).
24. J. B. S. Haldane, Sex ratio and unisexual sterility in hybrid animals. *J. Genet.* **12**, 101–109 (1922).
25. M. Schilthuizen, M. C. W. G. Giesbers, L. W. Beukeboom, Haldane's rule in the 21st century. *Heredity (Edinb)* **107**, 95–102 (2011).
26. M. Turelli, L. C. Moyle, Asymmetric postmating isolation: Darwin's corollary to Haldane's rule. *Genetics* **176**, 1059–1088 (2007).
27. J. P. Masly, D. C. Presgraves, High-resolution genome-wide dissection of the two rules of speciation in *Drosophila*. *PLoS Biol.* **5**, e243 (2007).
28. B. A. Payseur, J. G. Krenz, M. W. Nachman, Differential patterns of introgression across the X chromosome in a hybrid zone between two species of house mice. *Evolution* **58**, 2064–2078 (2004). Correction in: *Int. Org. Evolution* **59**, 474 (2005).
29. M. D. Carling, R. T. Brumfield, Haldane's rule in an avian system: Using cline theory and divergence population genetics to test for differential introgression of mitochondrial, autosomal, and sex-linked loci across the *Passerina* bunting hybrid zone. *Evolution* **62**, 2600–2615 (2008).
30. D. K. Herrig, A. J. Modrick, E. Brud, A. Llopart, Introgression in the *Drosophila subobscura–D. madeirensis* sister species: Evidence of gene flow in nuclear genes despite mitochondrial differentiation. *Evolution* **68**, 705–719 (2014).
31. A. Qvarnström, R. I. Bailey, Speciation through evolution of sex-linked genes. *Heredity (Edinb)* **102**, 4–15 (2009).
32. J. H. Malone, P. Michalak, Physiological sex predicts hybrid sterility regardless of genotype. *Science* **319**, 59 (2008).
33. C. Dufresnes *et al*., Empirical evidence for large X-effects in animals with undifferentiated sex chromosomes. *Sci. Rep.* **6**, 21029 (2016).
34. D. A. Filatov, The two "rules of speciation" in species with young sex chromosomes. *Mol. Ecol.* **27**, 3799–3810 (2018).
35. S. A. Frank, Divergence of meiotic-drive suppression systems as an explanation for sex-biased hybrid sterility and inviability. *Evolution* **45**, 262–267 (1991).
36. L. D. Hurst, A. Pomiankowski, Causes of sex ratio bias may account for unisexual sterility in hybrids: A new explanation of Haldane's rule and related phenomena. *Genetics* **128**, 841–858 (1991). Correction in: *Genetics* **129**, 603 (1991).
37. Y. Tao, D. L. Hartl, Genetic dissection of hybrid incompatibilities between *Drosophila simulans* and *D. mauritiana*. III. Heterogeneous accumulation of hybrid incompatibilities, degree of dominance, and implications for Haldane's rule. *Evolution* **57**, 2580–2598 (2003).
38. S. R. McDermott, M. A. F. Noor, The role of meiotic drive in hybrid male sterility. *Philos. Trans. R. Soc. Lond. B Biol. Sci.* **365**, 1265–1272 (2010).
39. C. I. Wu, A. W. Davis, Evolution of postmating reproductive isolation: The composite nature of Haldane's rule and its genetic bases. *Am. Nat.* **142**, 187–212 (1993).
40. C. I. Wu, N. A. Johnson, M. F. Palopoli, Haldane's rule and its legacy: Why are there so many sterile males? *Trends Ecol. Evol.* **11**, 281–284 (1996).
41. P. Nosil, J. L. Feder, Genomic divergence during speciation: Causes and consequences. *Philos. Trans. R. Soc. Lond. B Biol. Sci.* **367**, 332–342 (2012).
42. R. Burri *et al*., Linked selection and recombination rate variation drive the evolution of the genomic landscape of differentiation across the speciation continuum of *Ficedula* flycatchers. *Genome Res.* **25**, 1656–1665 (2015).
43. J. B. W. Wolf, H. Ellegren, Making sense of genomic islands of differentiation in light of speciation. *Nat. Rev. Genet.* **18**, 87–100 (2017).
44. D. L. Jeffries *et al*., A rapid rate of sex-chromosome turnover and non-random transitions in true frogs. *Nat. Commun.* **9**, 4088 (2018).
45. C. Dufresnes, A. Brelsford, F. Baier, N. Perrin, When sex chromosomes recombine only in the heterogametic sex: Heterochiasmy and heterogamety in *Hyla* tree frogs. *Mol. Biol. Evol.* **38**, 192–200 (2021).
46. J. H. Malone, B. E. Fontenot, Patterns of reproductive isolation in toads. *PLoS One* **3**, e3900 (2008).
47. S. K. Woodley, "Chemical signaling in amphibians" in *Neurobiology of Chemical Communication*, C. Mucignat-Caretta, Ed. (CRC Press/Taylor & Francis, Boca Raton, FL, 2014), chap. 8.
48. M. Vences, D. Wake, "Speciation, species boundaries and phylogeography of amphibians" in *Amphibian Biology, Vol. 6, Systematics*, H. H. Heatwole, M. Tyler, Eds. (Surrey Beatty & Sons, 2007), pp. 2613–2669.
49. K. C. Wollenberg Valero Jr *et al*., Patterns, mechanisms, and genetics of speciation in reptiles and amphibians. *Genes (Basel)* **10**, 646 (2019).
50. O. Drillon, G. Dufresnes, N. Perrin, P.-A. Crochet, C. Dufresnes, Reaching the edge of the speciation continuum: Hybridization between three sympatric species of tree frogs (*Hyla*). *Biol. J. Linn. Soc. Lond.* **126**, 743–750 (2019).
51. C. Dufresnes *et al*., Fifteen shades of green: The evolution of *Bufotes* toads revisited. *Mol. Phylogenet. Evol.* **141**, 106615 (2019).
52. C. Dufresnes, G. Mazepa, Hybridogenesis in water frogs. *eLS* **1**, 718–726 (2020).
53. T. Price, Sexual selection and natural selection in bird speciation. *Philos. Trans. R. Soc. Lond. B. Biol. Sci.* **353**, 251–260 (1998).
54. T. D. Price, M. M. Bouvier, The evolution of F1 postzygotic incompatibilities in birds. *Evolution* **56**, 2083–2089 (2002).
55. T. Price, *Speciation in Birds* (Roberts & Company Publishers, Greenwood Village, CO, 2008).
56. P. Pulido-Santacruz, A. Aleixo, J. T. Weir, Genomic data reveal a protracted window of introgression during the diversification of a Neotropical woodcreeper radiation. *Evolution* **74**, 842–858 (2020).
57. A. N. G. Kirschel *et al*., CYP2J19 mediates carotenoid colour introgression across a natural avian hybrid zone. *Mol. Ecol.* **29**, 4970–4984 (2020).
58. A. F. Kautt *et al*., Contrasting signatures of genomic divergence during sympatric speciation. *Nature* **588**, 106–111 (2020).
59. J. A. Coyne, H. A. Orr, Patterns of speciation in *Drosophila*. *Evolution* **43**, 362–381 (1989).
60. J. A. Coyne, H. A. Orr, "Patterns of speciation in *Drosophila*" revisited. *Evolution* **51**, 295–303 (1997).
61. R. Tingley, S. Dubey, Disparity in the timing of vertebrate diversification events between the northern and southern hemispheres. *BMC Evol. Biol.* **12**, 244 (2012).
62. S. B. Hedges, J. Marin, M. Suleski, M. Paymer, S. Kumar, Tree of life reveals clock-like speciation and diversification. *Mol. Biol. Evol.* **32**, 835–845 (2015).
63. T. Dobzhansky, Studies on hybrid sterility. II. Localization of sterility factors in *Drosophila pseudoobscura* hybrids. *Genetics* **21**, 113–135 (1936).
64. E. Mayr, *Systematics and the Origin of Species* (Columbia University Press, New York, 1942).
65. G. L. Stebbins, The inviability, weakness, and sterility of interspecific hybrids. *Adv. Genet.* **9**, 147–215 (1958).
66. P. Nosil, T. H. Vines, D. J. Funk, Perspective: Reproductive isolation caused by natural selection against immigrants from divergent habitats. *Evolution* **59**, 705–719 (2005).
67. M. E. Arnegard *et al*., Genetics of ecological divergence during speciation. *Nature* **511**, 307–311 (2014).
68. D. Schluter, Evidence for ecological speciation and its alternative. *Science* **323**, 737–741 (2009).
69. D. Bachtrog *et al*.; Tree of Sex Consortium, Sex determination: Why so many ways of doing it? *PLoS Biol.* **12**, e1001899 (2014).
70. J. F. Gerchen, C. Dufresnes, M. Stöck, Introgression across hybrid zones is not mediated by large X-effects in green toads with undifferentiated sex chromosomes. *Am. Nat.* **192**, E178–E188 (2018).
71. N. Perrin, Sex-chromosome evolution in frogs: What role for sex-antagonistic genes? *Philos. Trans. R. Soc. Lond. B Biol. Sci.* **376**, 20200094 (2021).
72. N. Rodrigues, T. Studer, C. Dufresnes, N. Perrin, Sex-chromosome recombination in common frogs brings water to the fountain-of-youth. *Mol. Biol. Evol.* **35**, 942–948 (2018). Correction in: *Mol. Biol. Evol.* **35**, 1821 (2018).
73. D. Macaya-Sanz *et al*., Genetic analysis of post-mating reproductive barriers in hybridizing European *Populus* species. *Heredity (Edinb)* **107**, 478–486 (2011).
74. K. Anderson, "Chromosome evolution in Holarctic *Hyla* treefrogs" in *Amphibian Cytogenetics and Evolution*, D. M. Green, S. K. Sessions, Eds. (Academic Press, San Diego, 1991), pp. 299–331.
75. C. Dufresnes *et al*., Sex-chromosome differentiation parallels postglacial range expansion in European tree frogs (*Hyla arborea*). *Evolution* **68**, 3445–3456 (2014).
76. D. C. Presgraves, H. A. Orr, Haldane's rule in taxa lacking a hemizygous X. *Science* **282**, 952–954 (1998).
77. T. G. Lima, Higher levels of sex chromosome heteromorphism are associated with markedly stronger reproductive isolation. *Nat. Commun.* **5**, 4743 (2014).
78. C. Dufresnes *et al*., Hybridization and introgression between toads with different sex chromosome systems. *Evol. Lett.* **4**, 444–456 (2020).
79. D. M. Hillis, Species delimitation in herpetology. *J. Herpetol.* **53**, 3–12 (2019).
80. D. M. Hillis, The detection and naming of geographic variation within species. *Herpetol. Rev.* **51**, 52–56 (2020).
81. K. de Queiroz, An updated concept of subspecies resolves a dispute about the taxonomy of incompletely separated lineages. *Herpetol. Rev.* **51**, 459–461 (2020).
82. C. Roux *et al*., Shedding light on the grey zone of speciation along a continuum of genomic divergence. *PLoS Biol.* **14**, e2000234 (2016).
83. A. J. Helbig, A. G. Knox, D. T. Parkin, G. Sangster, M. Collinson, Guidelines for assigning species rank. *Ibis* **144**, 518–525 (2002).
84. C. D. Jiggins, J. Mallet, Bimodal hybrid zones and speciation. *Trends Ecol. Evol.* **15**, 250–255 (2000).
85. M. Kirkpatrick, V. Ravigné, Speciation by natural and sexual selection: Models and experiments. *Am. Nat.* **159** (suppl. 3), S22–S35 (2002).
86. K. O. Chan *et al*., Species delimitation with gene flow: A methodological comparison and population genomics approach to elucidate cryptic species boundaries in Malaysian Torrent Frogs. *Mol. Ecol.* **26**, 5435–5450 (2017).
87. C. Fišer, C. T. Robinson, F. Malard, Cryptic species as a window into the paradigm shift of the species concept. *Mol. Ecol.* **27**, 613–635 (2018).
88. B. Hausdorf, C. Hennig, Species delimitation and geography. *Mol. Ecol. Resour.* **20**, 950–960 (2020).
89. X. Jiao, Z. Yang, Defining species when there is gene flow. *Syst. Biol.* **70**, 108–119 (2021).
90. C. Dufresnes *et al*., Integrating hybrid zone analyses in species delimitation: Lessons from two anuran radiations of the Western Mediterranean. *Heredity (Edinb)* **124**, 423–438 (2020).
91. C. Dufresnes, M. Berroneau, S. Dubey, S. N. Litvinchuk, N. Perrin, The effect of phylogeographic history on species boundaries: A comparative framework in *Hyla* tree frogs. *Sci. Rep.* **10**, 5502 (2020).
92. J. A. Tobias *et al*., Quantitative criteria for species delimitation. *Ibis* **152**, 724–746 (2010).
93. S. Kumar, G. Stecher, M. Li, C. Knyaz, K. Tamura, MEGA X: Molecular evolutionary genetics analysis across computing platforms. *Mol. Biol. Evol.* **35**, 1547–1549 (2018).
94. E. P. Derryberry, G. E. Derryberry, J. M. Maley, R. T. Brumfield, HZAR: Hybrid zone analysis using an R software package. *Mol. Ecol. Resour.* **14**, 652–663 (2014).
95. A. Brelsford, C. Dufresnes, N. Perrin, High-density sex-specific linkage maps of a European tree frog (*Hyla arborea*) identify the sex chromosome without information on offspring sex. *Heredity (Edinb)* **116**, 177–181 (2016).
96. C. Dufresnes, Phylogeography and hybrid zones of Palearctic amphibians. National Center for Biotechnology Information Sequence Read Archive. https://www.ncbi.nlm.nih.gov/bioproject/PRJNA542138. Deposited 9 May 2019.